Pergamon

Electrochimica Acta, Vol. 42, Nos 20–22, pp. 3327–3333, 1997

Printed in Great Britain
PII: S0013-4686(97)00184-9
0013–4686/97 $17.00 + 0.00

The scanning droplet cell and its application to structured nanometer oxide films on aluminium

A. W. Hassel* and M. M. Lohrengel

Institut für Physikalische Chemie und Elektrochemie II, Heinrich-Heine-Universität Düsseldorf, Universitätsstr. 1, 40225 Düsseldorf, Germany

Abstract—Structured oxide films were investigated with a scanning droplet cell. Different electrochemical techniques for surface analysis of valve metals (especially Al) are used. The electrolyte droplet had a diameter of some 100 μm. Impedance and potential sweep spectra are compared with current transients of pulse step experiments. The lateral resolution is limited to 1/10 of the droplet diameter. The normal resolution is better than 1 nm. © 1997 Published by Elsevier Science Ltd

Key words: Localisation, aluminium, anodic oxide, scanning droplet cell, electrochemical impedance spectroscopy, transients.

1. INTRODUCTION

The thickness of anodic, homogeneous aluminium oxide films is easily controlled by the formation potential in neutral solutions. The steady state thickness d depends on the formation potential according to

$$d = d_0 + kU, \quad (1)$$

where d_0 is a film thickness at 0 V and k is the formation factor which depends slightly on the formation conditions, *eg* formation time, temperature, and electrolyte. In our experiments an acetate buffer pH = 6.0 was used; under these conditions k is 1.6 nm V^{-1} for a potentiostatic formation for 1000 s and d_0 = 2.6 nm. The oxide film consists of amorphous Al_2O_3 from the barrier type with a density of 3.1 g cm^{-3} and a relative dielectric permittivity ε = 12 [1]. The initial film thickness is usually formed in wet air and, therefore, contains some water. In our experiments freshly electropolished specimens were used with a well defined initial thickness of d_0 = 1 nm, which is stable in the electrolyte for a few hours at a potential of −0.7 V (*hess*, hydrogen electrode in the same solution) [2]. Due to these properties this system is suitable for the preparation and analysis of structured oxide films in the nm-scale.

*Author to whom correspondence should be addressed. e-mail address: hassel@uni-duesseldorf.de.

2. EXPERIMENTAL

2.1 Electropolishing

The specimens were prepared from Aluminium sheets (99.95%, thickness 0.3 mm). To remove oxide films and to yield smooth surfaces the sheets were electropolished in mixtures of perchloric acid, methanole, 1,2-dimethoxyethane and 1-methoxyethanole at 225 K. This procedure guarantees mirror-like surfaces. To figure out the grain structure for experiments with the atomic force microscope some sheets were electropolished at much higher temperatures. At 300 K different grains are dissolved with different rates. As a result the grain boundaries are indicated by steps of some 100 nm.

2.2 Preparation of structured oxide films

To compare the different electrochemical techniques unsophisticated structures were used, *ie* a single step. Single steps in an oxide film on an aluminium sheet are effectively produced according to the following procedure [3]. The sheet is completely immersed and covered with an oxide film of the thickness d_1 at a potential U_1. Then the specimen is removed from the electrolyte and rinsed with clean water. After partial re-immersion additional oxide is formed at a higher potential U_2 in a second step. After removing and rinsing the sheet is ready for use.

2.3 Electronic set-up

The electronic equipment consisted of a fast rising potentiostat (rise time 0.3 μs), a pulse generator system for pulses and sweeps, a fast autoranging current detection system (switching time 1 μs), all in-house developments; and a Frequency Response Analyzer (Solatron Schlumberger 1255). Impedance measurements were recorded in the range 100 mHz $< f <$ 1 MHz with an *ac* amplitude of 10 mV.

The scanning droplet cell consisted of a polyethylene capillary (tip diameter 500 μm) which contained the reference electrode, the counter electrode and a step-motor controlled micro syringe (10 μl). Alternatively a gold capillary (diameter 150 μm) which served directly as a counter electrode was used. The complete droplet cell is mounted to a *x-y-z* stage (Isel Automation Eiterfeld) with a resolution of 5 μm. At a distance capillary/working electrode of about 100 μm an electrolyte droplet can be shifted to scan the surface. Due to the surface tension of the electrolyte droplet its diameter remains almost constant during the scan. Size and position of the droplet are continuously monitored by a video microscope. More details of this set-up will be described elsewhere [4].

3. INVESTIGATION TECHNIQUES

Common electrochemical techniques for an investigation of passive electrodes are impedance spectroscopy [5, 6], sweep techniques [7] and current transients of potentiostatic pulses [8]. All these techniques are combined and compared with the scanning droplet cell.

3.1 Impedance spectroscopy

Since the aluminium oxide behaves as an almost ideal dielectric material the corresponding equivalent circuit consists of only three components. The (uncompensated) electrolyte resistance R_Ω (some 10 Ω) is not of interest here. The oxide layer is described by the film resistance R_{0x} which represents the ionic conductivity, and the film capacity C connected in parallel. The differential film resistance [2] is given by:

$$R_{Ox} = \frac{d}{\beta i_0 \exp(\beta E)}, \tag{2}$$

where E is the field strength within the oxide and β and i_0 are oxide specific constants. The field strength E is calculated from the potential drop across the oxide.

$$E = \frac{\Delta U}{d} = \frac{U - U_0}{d}, \tag{3}$$

where $U_0 = -1.6$ V (*hess*) is the potential at which the field strength is zero. The oxide film capacity C is given by the plate condenser formula:

$$C = \frac{\epsilon_0 \epsilon}{d}. \tag{4}$$

Small deviations from this formula due to some dielectric relaxation phenomena [9, 10] are not considered in these experiments. The impedance spectra are given as Bode plots in the frequency range from 1 MHz to 0.1 Hz. Measurements down to much lower frequencies (10 μHz) were realised but not considered in this work due to the extreme periods of time needed for one spectrum.

3.2 Sweep techniques

Anodic potentiodynamic sweeps with a rate of 100 mVs^{-1} were recorded between 0 and 5 V (*hess*). The current increases rapidly if the potential exceeds the former film formation potential; the beginning of new oxide formation is characterised by its half-wave potential. This potential is some hundred mV higher than the preceding potentiostatic formation potential due to a kinetically delayed oxide formation [1, 11]. From the half-wave potentials the corresponding thicknesses are calculated. The current I is proportional to the electrode area. For structured surfaces the sweep spectrum is the sum of the spectra of the different surface parts. This analysis was introduced by Dunn [12].

3.3 Current transients of potentiostatic pulses

Due to the special oxide formation mechanism on some valve metals (Al, Nb, Ta) current transients of potentiostatic pulses show a specific shape. The time of the observed current maximum (overshoot) depends sensitively on the initial oxide thickness according to

$$t_{max} = \frac{d\rho}{i_0 \exp(\beta E)}, \tag{5}$$

where ρ is the concentration of mobile ions (*ca.* 100 C cm^{-3}). This method was successfully used to determine the porous structure of PVD (physical vapour deposition) [13] or cathodically damaged [14] oxide films. The current in the peak maximum is given by the common high-field-equation [11]

$$i_{max} = i_0 \exp(\beta E). \tag{6}$$

4. INVESTIGATION OF STRUCTURED OXIDES

4.1 Comparison of impedance, sweeps and pulse transients

Figure 1 compares spectra from impedance, sweep and pulse measurements for different structures and electrolyte droplet positions. In Fig. 1(a) a relatively high step $d_2 - d_1 = 3.2$ nm ($d_1 = 4.2$ nm, $d_2 = 7.4$ nm) was investigated. The droplet was positioned so that the centre of the contact area was just above the oxide step.

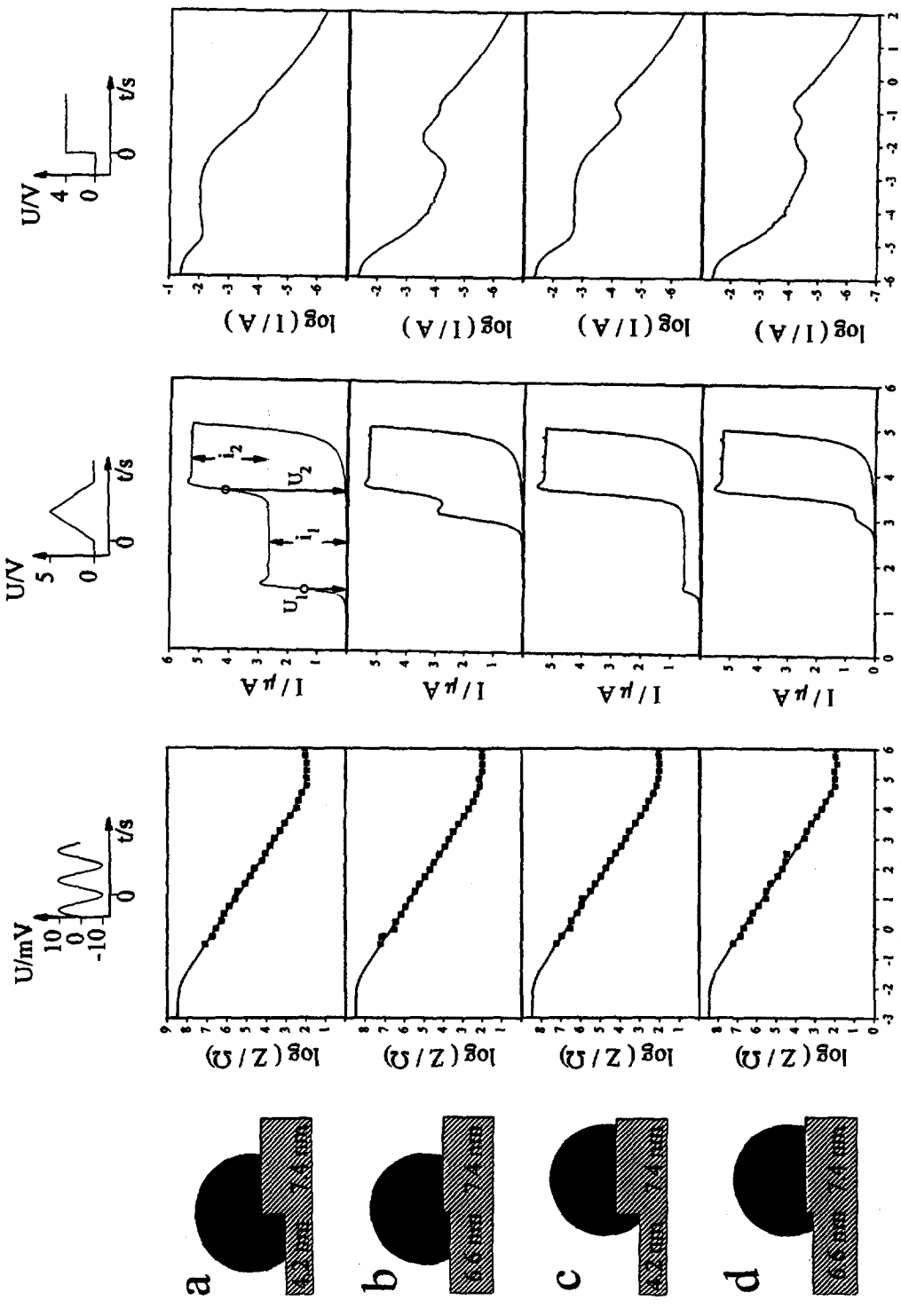

Fig. 1. Analysis of an oxide step on aluminium with the scanning droplet cell. Oxide step and droplet position (left column) are not true to scale. Comparison of impedance and sweep spectra and pulse transients. The results are presented in Tables 2 and 3

Table 1.
Geometrical parameters of the specimen, thicknesses of the oxide film d_1 and d_2 and ratio of the corresponding areas $A_1/(A_1 + A_2)$ in the experiments in Fig. 1

	d_1 (nm)	d_2 (nm)	$A_1/(A_1 + A_2)$
Fig. 1(a)	4.16	7.36	0.50
Fig. 1(b)	6.56	7.36	0.50
Fig. 1(c)	4.16	7.36	0.10
Fig. 1(d)	6.56	7.36	0.10

This is clearly seen in the sweep experiment. The current is close to zero until the potential I_1 corresponding to d_1, is exceeded. A constant current i_1 of oxide formation is observed. Later, if the potential exceeds U_2, the current increases again to $I_1 + I_2 = 2 \times I_1$ indicating that the areas with d_1 and d_2 are equal. Generally speaking the ratio of the surface parts with d_1 and d_2 is given by the plateau currents I_1 and I_2. The thicknesses can be calculated from sweeps with $dU/dt = 100$ mV s^{-1} according to

$$d = 1.8 \text{ nm} + 1.6 \text{ nm V}^{-1} \times U_n \qquad (7)$$

where U_n is the corresponding half-wave potential [15].

In all sweep experiments investigated here two steps were observed which are analysed in Table 2. The thicknesses were calculated from equation (7), the surface ratio from:

$$\frac{A_1}{A_1 + A_2} = \frac{I_1}{I_1 + I_2}. \qquad (8)$$

The correspondence is surprisingly good taking into account that the first step in Fig. 1(b) and 1(d) is less pronounced.

The pulse transients in Fig. 1 always show two peaks. The second peak in Fig. 1(a) and 1(b) is, however, difficult to separate. This indicates that small thicker areas are poorly resolved beneath larger thin areas. Due to the extremely high resolution the peak maximum for very thin layers (*eg* 4.2 nm Fig. 1(a) and 1(c)) should be shifted to very short times and large currents. This is not possible due to the limited potential control of the potentiostat and hence the shape of the peak changes to a delayed plateau. The peaks corresponding to 6.6 nm or 7.4 nm are well shaped and can be analysed. This is done in Table 3 where film thicknesses calculated from equation (5) are given. The ratio of the corresponding surfaces is evaluated from equation (5) and equation (6).

$$\frac{A_1}{A_2} = \frac{I_1 t_1}{I_2 t_2}, \qquad (9)$$

where I_1, I_2 and t_1, t_2 are the peak values of current and time, respectively. There is again a quite good correspondence to the values of Table 1 indicating, that a surface analysis by sweeps or transients is almost equivalent. The sweep experiments are slightly more precise, one advantage of the transient technique is the separation of small thin parts beneath larger thick areas.

So far the Bode plots in Fig. 1 are not considered. In fact, the differences of the spectra are small. Only one time constant is observed in our cases. The capacity decreases slightly in the sequence $C_a > C_c > C_b > C_d$. This behaviour is expected from the equivalent circuit. The two capacities according to d_1 and d_2 are connected in parallel since the electrolyte interface represents an

Table 2.
Analysis of the sweep experiments in Fig. 1, half wave potentials U_1 and U_2 and the corresponding plateau currents I_1 and $I_1 + I_2$. The thicknesses were calculated from equation (7)

	U_1 (V)	I_1 (A)	U_2 (V)	$(I_1 + I_2)$ (A)	d_1 (nm)	d_2 (nm)	$A_1/(A_1 + A_2)$
Fig. 1(a)	1.36	2.67	3.52	5.25	3.97	7.43	0.50
Fig. 1(b)	2.90	2.80	3.52	5.33	6.44	7.43	0.53
Fig. 1(c)	1.35	0.55	3.50	5.29	3.96	7.40	0.10
Fig. 1(d)	2.92	0.67	3.51	5.29	6.47	7.41	0.12

Table 3.
Analysis of the transient experiments in Fig. 1, current and time maxima of the peaks. Surface ratios were calculated from equation (8), thicknesses from equation (5)

	I_1 (A)	t_1 (s)	I_2 (A)	t_2 (s)	$I_1 t_1/(I_1 t_1 + I_2 t_2)$	d_1 (nm)	d_2 (nm)
Fig. 1(a)	1.00×10^{-2}	6.03×10^{-4}	2.92×10^{-5}	1.86×10^{-1}	0.53	(<6)	7.24
Fig. 1(b)	2.95×10^{-4}	1.58×10^{-2}	2.81×10^{-5}	1.86×10^{-1}	0.47	6.61	7.24
Fig. 1(c)	1.86×10^{-3}	4.37×10^{-4}	7.17×10^{-5}	1.86×10^{-1}	0.06	(<6)	7.24
Fig. 1(d)	7.08×10^{-5}	1.58×10^{-2}	7.05×10^{-5}	1.86×10^{-1}	0.08	6.61	7.24

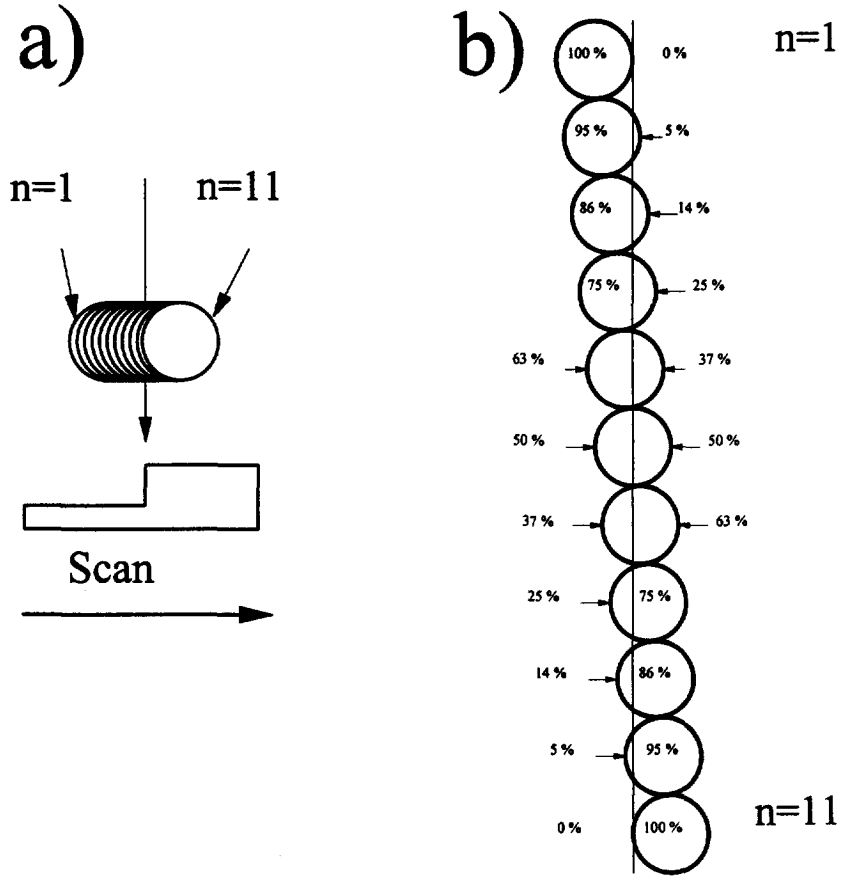

Fig. 2. Relative positions of oxide step and droplet during a scan, (a) non-destructive techniques like impedance spectroscopy (b) techniques, which require additional oxide formation

equipotential plane. Therefore only the mean capacity is measured.

4.2 Structure analysis by locally resolved impedance spectroscopy

A detection of surface structures becomes possible by impedance if a sequence of measurements at different positions is done. An advantage of this technique is the possibility to record several spectra at the same position without changing the thickness of the film. Thus, overlapping spots can be measured as shown in Fig. 2(a). As a result the impedance at 1 kHz (referring to the reciprocal capacity) is plotted vs the position in Fig. 3 (rectangles). The resolution seems to be limited to the drop diameter. Due to the overlapping parts the information of the investigated areas is included in subsequent measurements. This information can be extracted from the set of data using successive differences. Details of this method will be described elsewhere [16]. The result of this defolding procedure is also shown in Fig. 3 (circles). The lines show the expected behaviour of the impedance before (dashed line) and after smearing out by the droplet (full line).

4.3 Locally resolved sweep spectra

The principle of analysis by sweep spectra is a formation of additional oxide, therefore only one measurement is possible at a given position. Overlapping spots as in Fig. 2(a) must be avoided

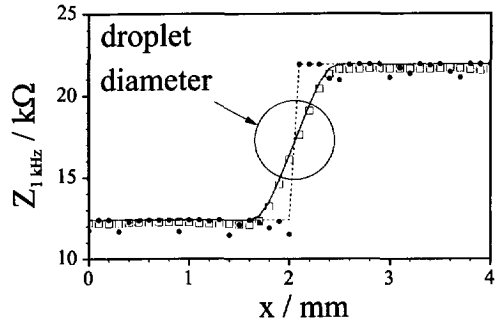

Fig. 3. The reciprocal capacity (impedance at 1 kHz) from impedance spectra vs position of a scan across an oxide step from 4.2 to 7.4 nm, measurements of the mean impedance (rectangles), data from the defolding procedure (circles), idealised oxide step (dashed line) and expected behaviour of the mean impedance (full line). For comparison the diameter of the scanning droplet (800 μm) is given as an insert

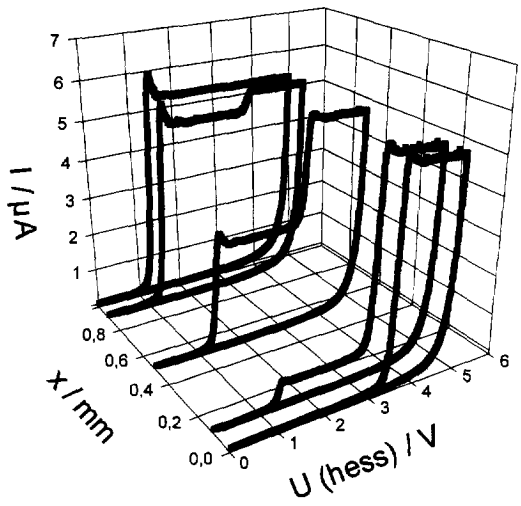

Fig. 4. Sweep spectra with $dU/dt = 100$ mV s^{-1} at different positions of a scan across an oxide step from 4.2 to 7.4 nm as in Fig. 2(b)

and a spot sequence as in Fig. 2(b) must be used. This technique requires to affect a larger area of the investigated surface. Figure 4 shows 5 sweep spectra for 5 different relative positions drop/step. A complex defolding procedure as in Section 4.2 is not necessary since the complete data (thickness and area ratio) can be taken from every sweep. The resolution is not determined by the droplet size but mainly by the "contrast" d_2/d_1 and by the ratio of the affected areas. Under our conditions a thickness difference of about 0.5 nm (or 300 mV) and a ratio of the corresponding areas of about 0.05 is resolved. Hence, the resolution is about one decade higher than the droplet diameter.

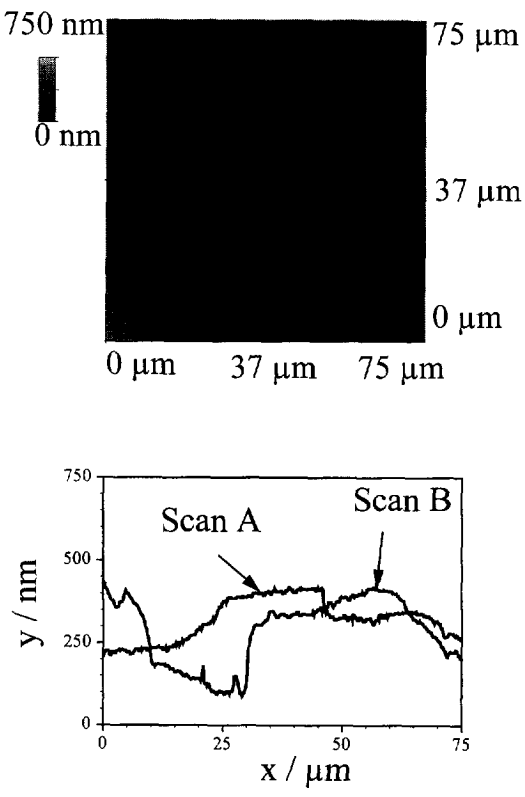

Fig. 5. Grain structure of an aluminium sheet after a special electropolishing procedure, surface image (a) and two line scans (b) recorded by an atomic force microscope

4.4 Atomic force microscopy

Electrochemical experiments, as presented here, can be influenced by the grain structure of the aluminium sheets. After a special electropolishing technique (Section 2.1) the grain boundaries form steps of some 100 nm and were investigated with the atomic force microscope (Topometrix TMX2000 Discoverer). Figure 5 shows a surface image. A mean grain size of 50 µm was estimated. This means that the resolution of the droplet in the version presented here is not sufficient for an investigation of single grains. Nevertheless the sweep and transient techniques enabled us to analyse a distribution of thicknesses in one experiment. No artefacts of different grains were found. Thus, a uniform oxide formation on an electropolished aluminium sheet must be assumed, independently of the grain structure.

5. SUMMARY

Spatially resolved surface analysis of oxide covered metals (here Al) becomes possible using the scanning droplet cell. Impedance and potential sweep spectra are compared with current transients of pulse step experiments. The sweep spectra and current transients give detailed information on the structure of the area determined by the electrolyte droplet. The normal resolution is much better than 1 nm for oxide thicknesses up to 10 or 20 nm. Disadvantageous is a modification of the investigated area because both techniques form additional oxide. From impedance data a separation of parts of different thickness is not possible from one spectrum since mean capacities and mean resistivities of the wetted area are always determined. One advantage of this method, however, is the non-destructive measurement, *ie* the oxide thicknesses are not affected. Therefore the lateral resolution can be enhanced by the method of successive differences. As a result, the resolution is almost equal to the values of sweep and transient techniques, about 1/10 of the droplet diameter *ie* 15 µm.

ACKNOWLEDGEMENTS

The financial support of the Deutsche Forschungsgemeinschaft and the Wissenschaftsministerium des Landes Nordrhein-Westfalen is gratefully acknowledged. The authors wish to thank O. Voigt for the AFM analysis.

REFERENCES

1. A. W. Hassel, M. M. Lohrengel, S. Rüße and J. W. Schultze, *Bull. Chem. Technol. Maced.* **13,** 49 (1994).
2. A. W. Hassel and M. M. Lohrengel, *Mater. Sci. Forum* **185**(188), 581 (1995).
3. M. M. Lohrengel and S. Rüße, *Mater. Sci. Forum* **185–188,** 611 (1995).
4. A. W. Hassel and M. M. Lohrengel, **in preparation.**
5. J. R. Macdonald, *Impedance Spectroscopy*, John Wiley, New York (1987).
6. M. Sluyters-Rehbach, *Pure Appl. Chem.* **66,** 1831 (1994).
7. A. J. Bard, L. R. Faulkner, *Electrochemical Methods. Fundamentals and Applications*, John Wiley, New York (1980).
8. M. M. Lohrengel, *Ber. Bunsen-Ges. Phys. Chem.* **97,** 440 (1993).
9. A. K. Jonscher, *Phys. Status Solidi B* **83,** 585 (1977).
10. S. Rüße, M. M. Lohrengel and J. W. Schultze, *Solid State Ionics* **72,** 29 (1994).
11. M. M. Lohrengel, *Mater. Sci. Eng. R* **11,** 243 (1993).
12. C. G. Dunn and L. A. Harris, *J. Electrochem. Soc.* **11,** 81 (1970).
13. D. Diesing, S. Rüße and M. M. Lohrengel, in *Electroceramics IV Proc.* **Vol. II**, (1994) 1295.
14. A. W. Hassel and M. M. Lohrengel, *Electrochim. Acta* **40,** 433 (1995).
15. L. Meites, P. Zuman and H. W. Nürnberg, *Pure Appl. Chem.* **57,** 1491–1505 (1985).
16. A. W. Hassel, **in preparation.**